An Ultrasensitive Flexible Pressure, Temperature, and Humidity Sensor Based on Structurally Adjustable Nano-through-hole Array Films

Shuang Xiao[1, 2, 3], Yin He[1, 2, 3*], Yawen Lu[5], Xin Niu[1, 2, 3], Qianqian Li[3], Junxian Wu[2], Dan Luo[1, 2, 3], Fujun Tian[2], Gang Wan[4] and Hao Liu[1, 2, 3*]

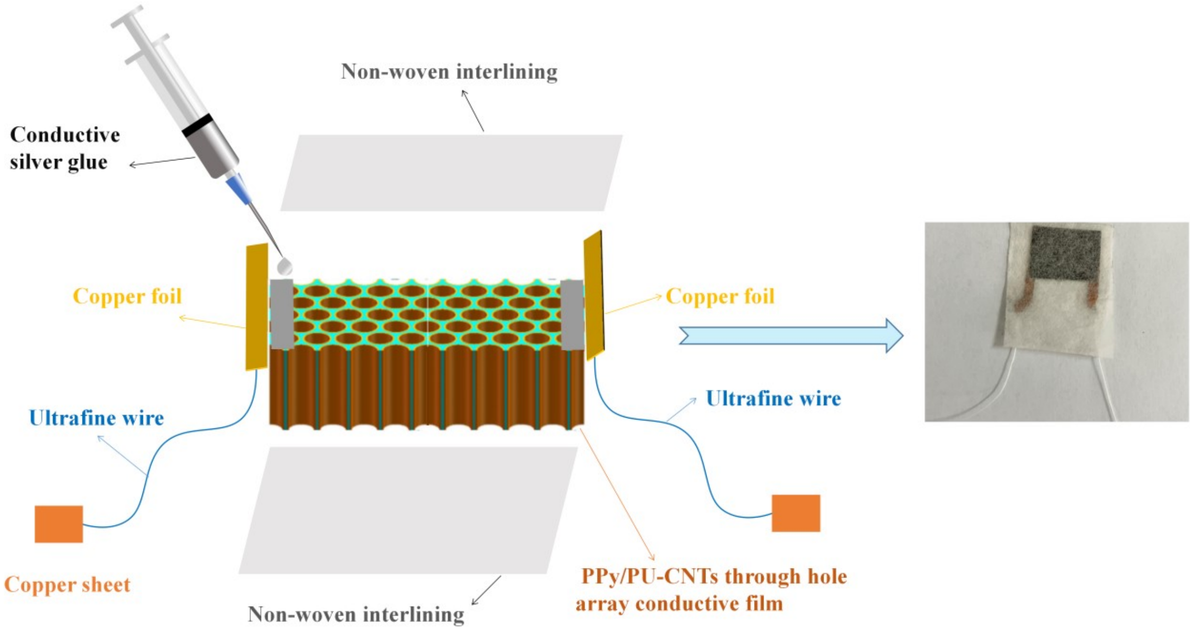

Figure S1. Based on PPy/PU-CNTs nano-through-hole conductive film flexible multiresponsive sensors packaging process diagram.

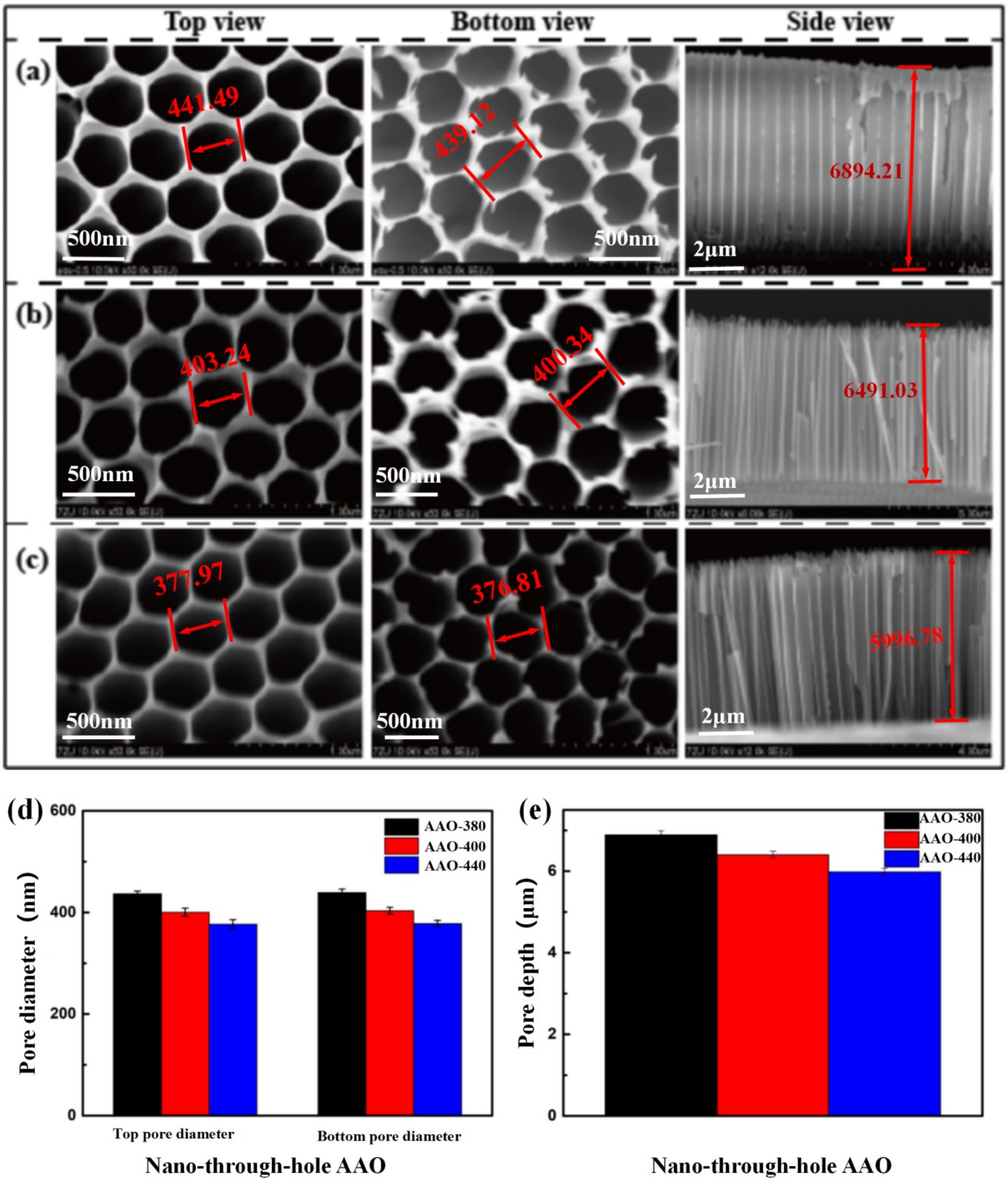

Figure S2. SEM images of three kinds of nano-through-hole AAO formwork (AAO-440, AAO-400 and AAO-380). **a)** SEM images of AAO-440. **b)** SEM images of AAO-400. **c)** SEM images of AAO-380. **d)** The pore diameter of three kinds of nano-through-hole AAO. **e)** The pore depth of three kinds of nano-through-hole AAO.

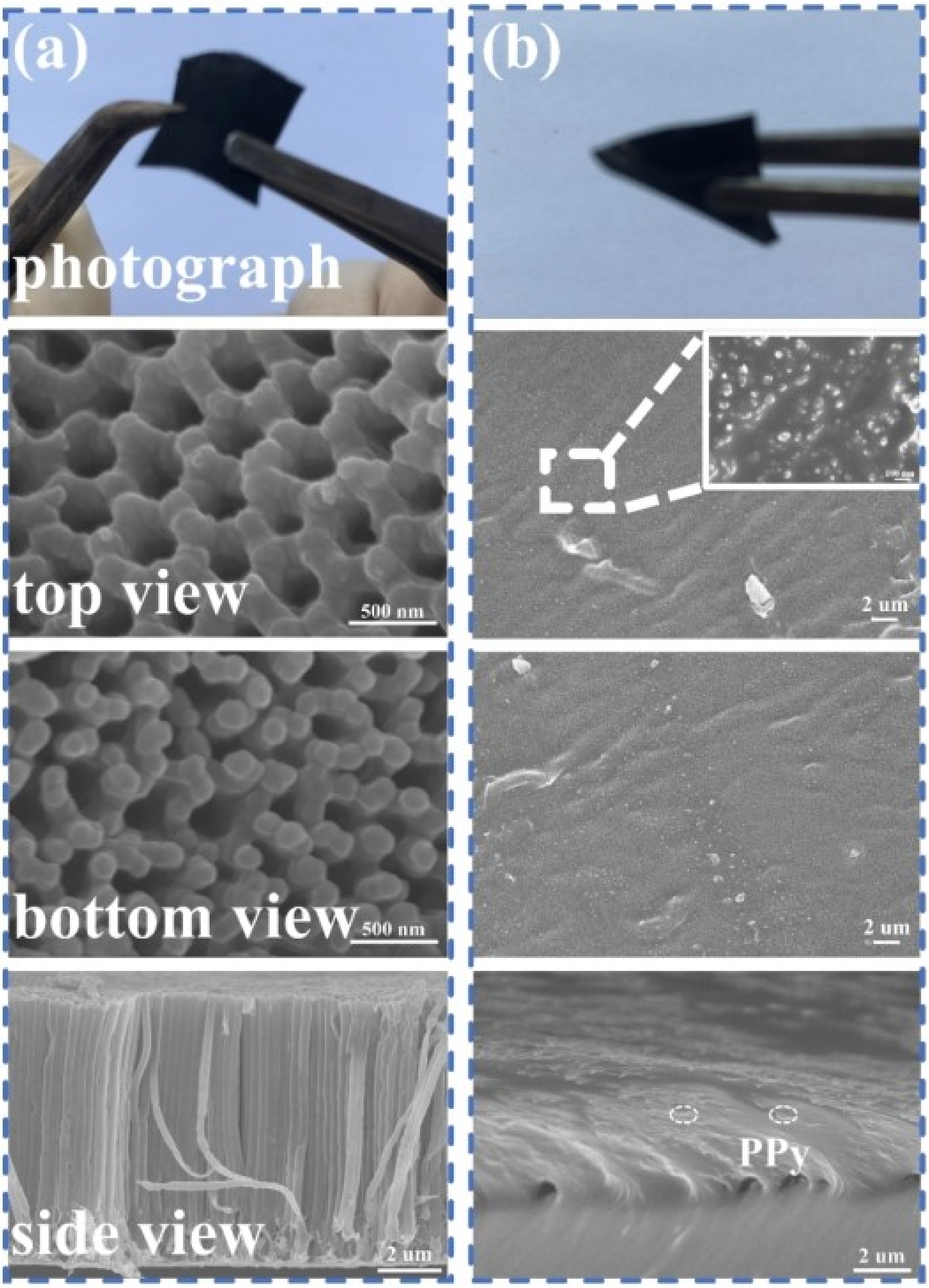

Figure S3. SEM images of PPy/PU-CNTs nano-through-hole conductive film and PPy/PU-CNT planar conductive film. **a)** SEM images of the nano-through-hole array conductive film. **b)** SEM images of the planar conductive film.

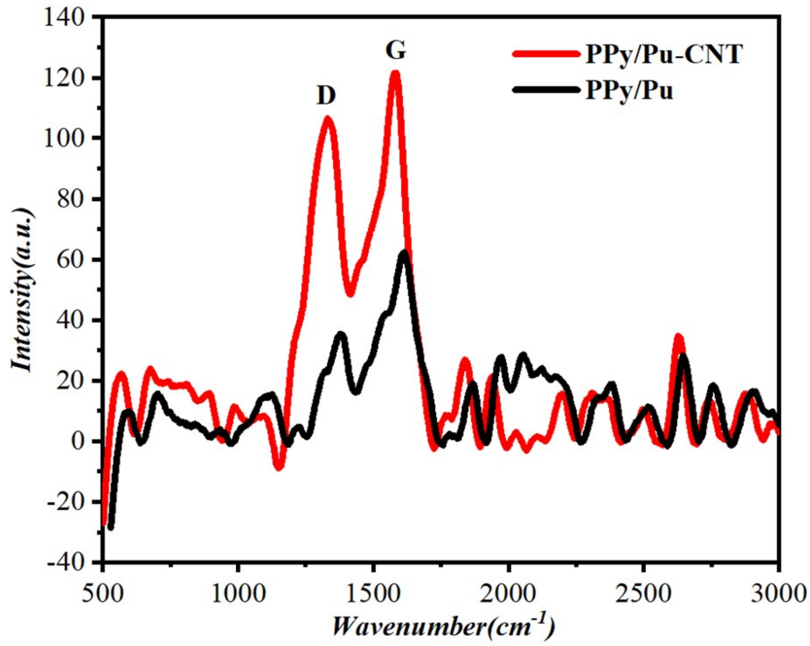

Figure S4. Raman spectra of PPy/PU-CNTs nano-through-hole film and PPy/PU film.

Table S1. Sensitivity of PPy/PU-CNTs multiresponsive sensors in a certain temperature range

Temperature	20-50 ℃	50-80 ℃
Hole-380 sensor Sensitivity（%℃$^{-1}$）	0.51	0.44
Hole-400 sensor Sensitivity（%℃$^{-1}$）	0.56	0.66
Hole-440 sensor Sensitivity（%℃$^{-1}$）	0.72	0.58

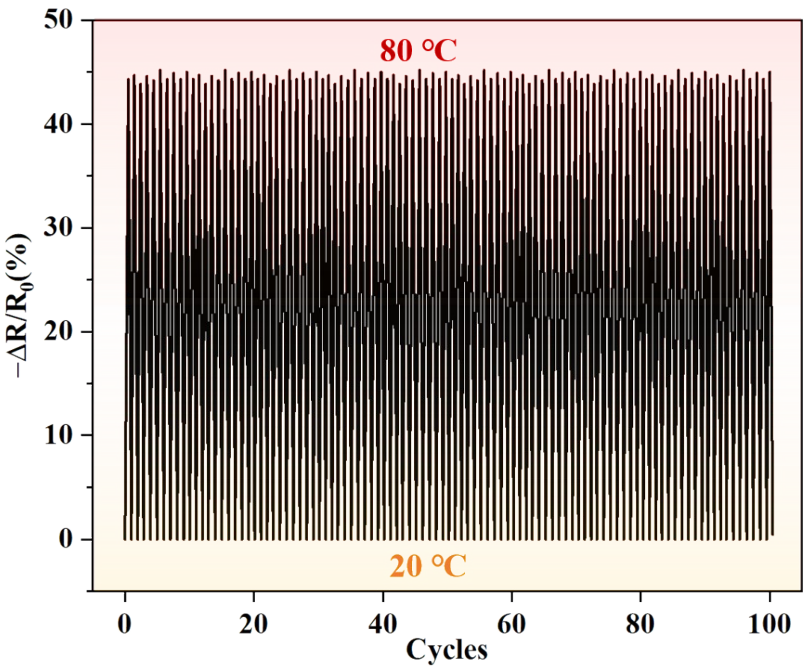

Figure S5. The resistance change rate image of the Hole-440 sensor during 100 cycles of heating and cooling at temperatures range from 20 °C to 80 °C.

Table S2. Humidity sensitivity of PPy/PU-CNTs multiresponsive sensors in a certain humidity range

Humidity（RH%）	20	35	50	65	80
Hole-380 sensor Sensitivity（$\%RH^{-1}$）	0.18	0.26	0.49	0.68	1.28
Hole-400 sensor Sensitivity（$\%RH^{-1}$）	0.13	0.19	0.40	0.82	1.71
Hole-440 sensor Sensitivity（$\%RH^{-1}$）	0.19	0.32	0.57	1.33	3.51

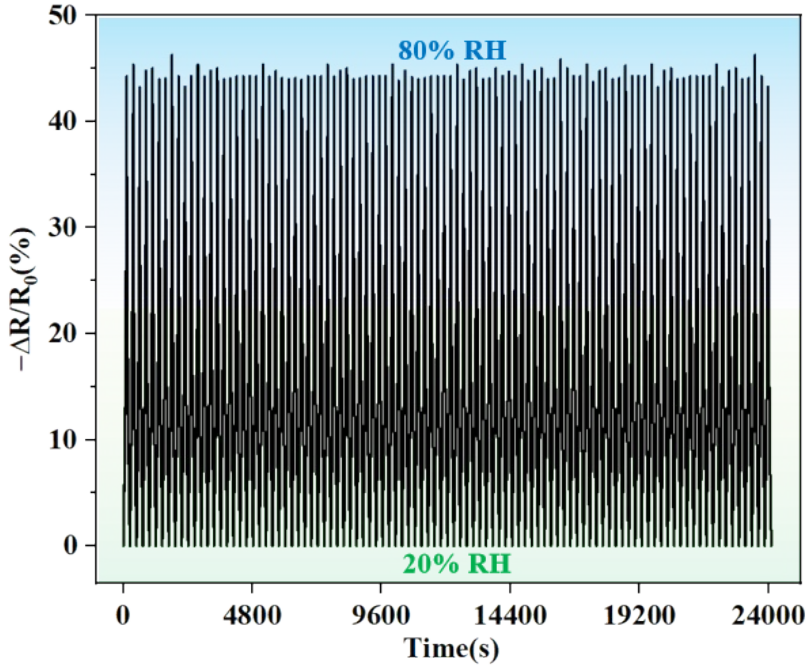

Figure S6. The resistivity change rate image of Hole-440 sensor during 100 loading and unloading cycles under humidity of 20–80% RH.

Table S3. Sensitivity of PPy/PU-CNT multiresponsive sensors in a certain pressure range (kPa^{-1})

Pressure	0.2 kPa	0.5 kPa	1 kPa	5 kPa	12 kPa
Hole-380 sensor Sensitivity（kPa^{-1}）	102.99	85.84	64.57	16.10	7.15
Hole-400 sensor Sensitivity（kPa^{-1}）	72.66	55.6	12.26	3.02	0.78
Hole-440 sensorSensitivity（kPa^{-1}）	42.55	27.81	11.66	3.67	0.71

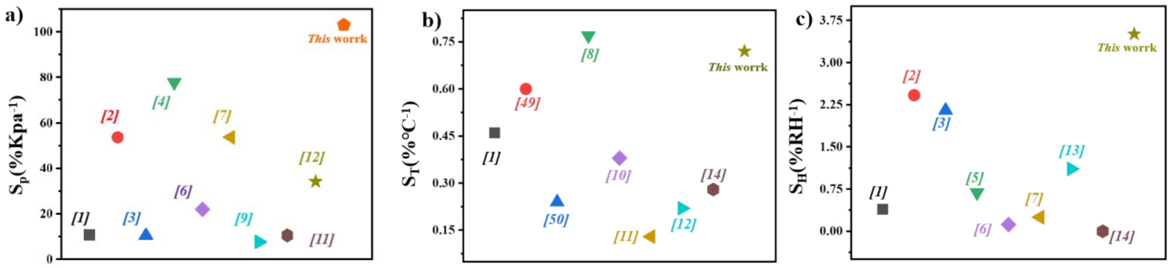

Figure S7. comparing the sensitivity of recently reported flexible multi-response sensors：**(a)** pressure response sensitivity comparison; **(b)** temperature response sensitivity comparison; **(c)** humidity response sensitivity comparison

Table S4. Comparison of recent reported flexible multiresponsive sensors.

Active material	Electrical response signal	Sensitivity S_P S_T S_H	Range Pressure Temperature Humidity	Reference
Organohydrogel based on hyaluronic acid and poly (acrylic acid-co-acrylamide)	Resistance	10.79%kpa^{-1} 0.46%℃$^{-1}$ 0.39%RH^{-1}	0-800%Strain 25-100℃ 11-98%RH	[1]
Carbon nanotube-polydimethylsiloxane	Resistance	53.7%kpa^{-1} / 2.42%RH^{-1}	0-50kpa / 15-85%RH	[2]
Citric acid (CA) and sodium polystyrene sulfonate (PSS)-thermoplastic polyurethane	Resistance	10.53%kpa^{-1} / 2.15%RH^{-1}	0-26kpa / 20-90%RH	[3]
Single-walled carbon nanotubes/polydimethylsiloxane mixture	Resistance	77.78%kpa^{-1} / 11.145%RH^{-1}	0.024-230kpa / 25-80%RH	[4]
Nickel networks on polyurethane sponge	Resistance	2.576%kpa^{-1} 1.77%℃$^{-1}$ 0.69%RH^{-1}	0.1-12kpa 20-100℃ 11-97%RH	[5]
Soak-drying Melamine foam with the conducting aqueous RGO-CNT ink	Resistance	22%kpa^{-1} 0.6%℃$^{-1}$ 0.12%RH^{-1}	0-5kpa -7-140℃ 25-82%RH	[6]
Silver nanowires, carbon nanotubes, zinc oxide, and 3,4-ethylenedioxythiophene polystyrene sulfonate	Resistance	53.7%kpa^{-1} 0.24%℃$^{-1}$ 0.25%RH^{-1}	0-180kpa 0-25℃ 0-40%RH	[7]
poly(3,4-ethylenedioxythiop)hene:poly(styrenesulfonate) (3-glycidyloxypropyl)	Resistance	/ 0.77%℃$^{-1}$ /	/ 25-50℃ /	[8]
Single-walled carbon nanotubes/polydimethylsilox	Resistance	7.76%kpa^{-1} / /	0-400kpa / /	[9]
piezoelectric polyvinylidene fluoride nanofibrous membrane doped with zinc oxide nanoparticles carbon nanofibers	Resistance	/ 0.38%℃ /	4.9-45kpa 25-100℃ /	[10]
Polydimethylsiloxane film embeddedwith single-walled carbon nanotubes and a polyimide film	Resistance	10.6%kpa^{-1} 0.13%℃$^{-1}$ /	0-3.2kpa 25-105℃ /	[11]
MXene (Ti3C2Tx) colloidal flexible polyurethane foam	Resistance	34.24%kpa^{-1} 0.22%℃$^{-1}$ /	1.47-3.16kpa 25-100℃ /	[12]
laser-induced graphene (LIG) and graphene oxide (GO）	Resistance	/ / 1.11%RH^{-1}	/ / 11-97%RH	[13]
Laser-induced graphene (LIG) produced by irradiation of paper	Resistance	/ 0.28%℃$^{-1}$ 0.001%RH^{-1}	/ 10-60℃ 23-85%RH	[14]
Polypyrrole/polyurethane-carbon nanotubes	Resistance	102.99%kpa^{-1} 0.72%℃$^{-1}$ 3.51%RH^{-1}	0-12kpa 20-80℃ 20-80%RH	This work

References

[1] B. Chethan, H.G.R. Prakash, Y.T. Ravikiran, S.C. Vijayakumari, S. Thomas, Polypyyrole based core-shell structured composite based humidity Sensor operable at room temperature, Sensors and Actuators B: Chemical. 296 (2019) 126639. https://doi.org/10.1016/j.snb.2019.126639.

[2] L. Miao, J. Wan, Y. Song, H. Guo, H. Chen, X. Cheng, H. Zhang, Skin-Inspired Humidity and Pressure Sensor with a Wrinkle-on-Sponge Structure, ACS Appl. Mater. Interfaces. 11 (2019) 39219–39227. https://doi.org/10.1021/acsami.9b13383.

[3] S. Ding, Y. Lou, Z. Niu, J. Wang, X. Jin, J. Ma, B. Wang, X. Li, A Highly Sensitive, Breathable, and Biocompatible Wearable Sensor Based on Nanofiber Membrane for Pressure and Humidity Monitoring, Macro Materials & Eng. 307 (2022) 2200233. https://doi.org/10.1002/mame.202200233.

[4] C. Yang, A. Abodurexiti, X. Maimaitiyiming, Flexible Humidity and Pressure Sensors Realized by Molding and Inkjet Printing Processes with Sandwich Structure, Macromol. Mater. Eng. 305 (2020) 2000287. https://doi.org/10.1002/mame.202000287.

[5] J. Tong, N. Wang, Q. Wang, S. Chen, B. Sheng, Improved sensitive conductive sponge sensors with tunnel-crack broadening for pressure, humidity and temperature sensing applications, Sensors and Actuators B: Chemical. 358 (2022) 131497. https://doi.org/10.1016/j.snb.2022.131497.

[6] B.B. Bhatt, L. Kumar, A. Kushwaha, D. Gupta, An ultra-compressible piezoresistive strain and pressure sensor based on RGO-CNT-Melamine foam composite for biomedical sensing, Sensors and Actuators A: Physical. 331 (2021) 112875. https://doi.org/10.1016/j.sna.2021.112875.

[7] H.S. Jo, C.-W. Park, S. An, A. Aldalbahi, M. El-Newehy, S.S. Park, A.L. Yarin, S.S. Yoon, Wearable multifunctional soft sensor and contactless 3D scanner using supersonically

sprayed silver nanowires, carbon nanotubes, zinc oxide, and PEDOT:PSS, NPG Asia Mater. 14 (2022) 23. https://doi.org/10.1038/s41427-022-00370-y.

[8] Y.-F. Wang, T. Sekine, Y. Takeda, K. Yokosawa, H. Matsui, D. Kumaki, T. Shiba, T. Nishikawa, S. Tokito, Fully Printed PEDOT:PSS-based Temperature Sensor with High Humidity Stability for Wireless Healthcare Monitoring, Sci Rep. 10 (2020) 2467. https://doi.org/10.1038/s41598-020-59432-2.

[9] A. Abodurexiti, C. Yang, X. Maimaitiyiming, High-Performance Flexible Pressure and Temperature Sensors with Complex Leather Structure, Macromol. Mater. Eng. 305 (2020) 2000181. https://doi.org/10.1002/mame.202000181.

[10] Y. Wang, M. Zhu, X. Wei, J. Yu, Z. Li, B. Ding, A dual-mode electronic skin textile for pressure and temperature sensing, Chemical Engineering Journal. 425 (2021) 130599. https://doi.org/10.1016/j.cej.2021.130599.

[11] Y. Su, K. Ma, X. Zhang, M. Liu, Neural Network-Enabled Flexible Pressure and Temperature Sensor with Honeycomb-like Architecture for Voice Recognition, Sensors. 22 (2022) 759. https://doi.org/10.3390/s22030759.

[12] V. Adepu, V. Mattela, P. Sahatiya, A remarkably ultra-sensitive large area matrix of MXene based multifunctional physical sensors (pressure, strain, and temperature) for mimicking human skin, J. Mater. Chem. B. 9 (2021) 4523–4534. https://doi.org/10.1039/D1TB00947H.

[13] X. Yao, L. Chen, Z. Luo, C. Ye, F. Liang, T. Yang, X. Liu, X. Tian, H. Bi, C. Wang, C. Cai, L. Lyu, X. Wu, High-performance flexible humidity sensors for breath detection and non-touch switches, Nano Select. 3 (2022) 1168–1177. https://doi.org/10.1002/nano.202100343.

[14] B. Kulyk, B.F.R. Silva, A.F. Carvalho, P. Barbosa, A.V. Girão, J. Deuermeier, A.J.S. Fernandes, F.M.L. Figueiredo, E. Fortunato, F.M. Costa, Laser-Induced Graphene from

Paper by Ultraviolet Irradiation: Humidity and Temperature Sensors, Adv Materials Technologies. 7 (2022) 2101311. https://doi.org/10.1002/admt.202101311.